EUROPEAN ORGANIZATION FOR NUCLEAR RESEARCH

DESY/97-129
L3 note 2085
May 1997

Higgs Boson Searches at LEP

André Sopczak
DESY – Zeuthen *

Abstract

The latest LEP1 results from searches for the Higgs boson of the Minimal Standard Model (MSM), and for neutral and charged Higgs bosons of non-minimal Higgs models are reviewed from the four LEP experiments at CERN: ALEPH, DELPHI, L3, and OPAL. A total of about 16 million hadronic Z decays were recorded between 1989 and 1995 at the Z resonance. Much progress has been made due to the analysis of new data sets. Preliminary results of Higgs boson searches at LEP2 are presented.

Presented at the XII Int. Symposium on High Energy Physics, Gauhati, India, Dec. 26, 1996 to Jan. 2, 1997

*E-mail: andre.sopczak@cern.ch

Higgs Boson Searches at LEP

André Sopczak[a] *

[a]DESY – Zeuthen

The latest LEP1 results from searches for the Higgs boson of the Minimal Standard Model (MSM), and for neutral and charged Higgs bosons of non-minimal Higgs models are reviewed from the four LEP experiments at CERN: ALEPH, DELPHI, L3, and OPAL. A total of about 16 million hadronic Z decays were recorded between 1989 and 1995 at the Z resonance. Much progress has been made due to the analysis of new data sets. Preliminary results of Higgs boson searches at LEP2 are presented.

1. Introduction

The first Z boson was registered on August 13, 1989 at LEP1, and after about six years of data-taking at the Z resonance, large data sets with increasing luminosity were recorded each year. In 1994, the design luminosity was exceeded with more than 1.6 million hadronic Z boson decays recorded per experiment. In 1995, the LEP1 machine was upgraded for higher center-of-mass energies (LEP2) and started data-taking above the Z resonance. The integrated luminosity delivered to each LEP experiment is shown in Table 1. In 1997, LEP2 will run at about 184 GeV, and at a later stage, higher energies will be reached [1].

The large data set allows one of the most challenging quests of experimental particle physics to be pursued: the search for Higgs particles [2]. The experimental evidence of Higgs bosons is crucial for understanding the mechanisms of SU(2) × U(1) symmetry breaking and the mass generation in gauge theories. The Higgs mass is a free parameter in the MSM. Unlike the top, measurements of the Z-lineshape have very low precision for the Higgs mass, as illustrated in Fig. 1 (from [3]).

This article reviews the search for the MSM Higgs (Sec. 2), and the search for non-minimal Higgs bosons (Sec. 3). Interpretations are summarized based on the two-doublet Higgs model (Sec. 4) and the Minimal Supersymmetric Standard Model (MSSM) (Sec. 5). Preliminary results at LEP2 energies are presented (Sec. 6). Previous reports are given for example in [4, 5].

Table 1
Integrated luminosities delivered to each LEP experiment.

Year	1990	1991	1992	1993	1994	1995
$\mathcal{L}(\mathrm{pb}^{-1})$	7.6	17.3	28.6	40.0	64.5	40.0
Year	1995	1995	1995	1996	1996	1996
$\sqrt{s}$(GeV)	130	136	140	161	170	172
$\mathcal{L}(\mathrm{pb}^{-1})$	2.7	2.5	0.1	10.0	1.1	10.9

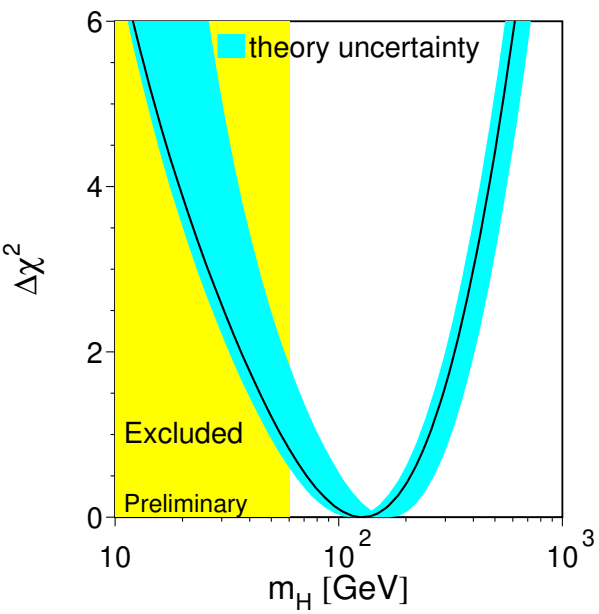

Figure 1. χ^2-fit on the Higgs boson mass from Z-lineshape measurements in the MSM. The upper mass limit, including the theoretical uncertainty, is 550 GeV at 95% CL.

*e-mail: andre.sopczak@cern.ch

2. MSM Higgs Search

The expected Higgs boson event rate [6] for the bremsstrahlung process [7] is known to better than 1%, including radiative corrections [8]. The expected number of Higgs boson events per 1 million hadronic Z decays is shown in Fig. 2.

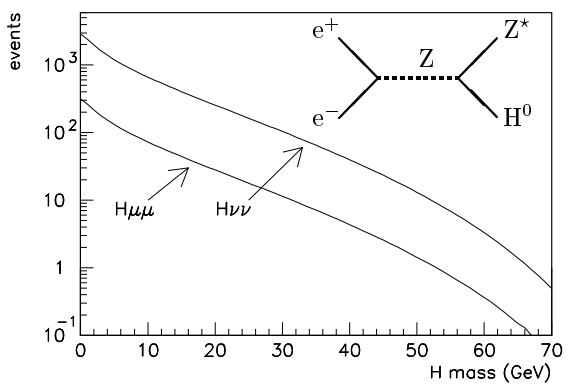

Figure 2. MSM Higgs production rate as a function of the Higgs boson mass.

The Higgs and Z decay modes determine the event signature in the detectors. Higgs bosons with low masses decay into e^+e^- and $\mu^+\mu^-$ pairs, for intermediate masses they decay into light hadrons and $\tau^+\tau^-$ pairs, and for high masses they decay predominantly into $b\overline{b}$ pairs.

2.1. High-Mass Higgs Bosons

The Z decay mode characterizes the search channel. The leptonic channels are very important because of their distinct topologies. The hadronic channel $Z \rightarrow Z^\star H \rightarrow q\overline{q}H$ is not used at LEP1 due to large QCD background. Typical Higgs event signatures are illustrated in Fig. 3.

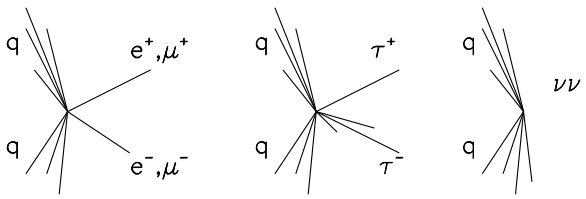

Figure 3. Schematic views of high-mass Higgs event topologies in the leptonic channels.

Expected signal efficiencies and background rates are shown for the neutrino channel in Fig. 4 (from [9]).

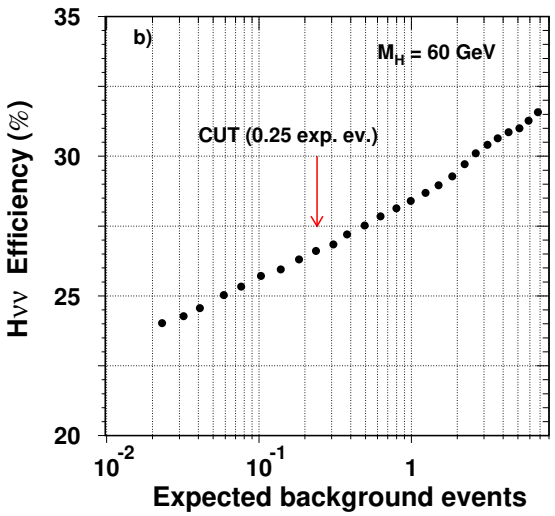

Figure 4. L3: $H\nu\nu$ detection efficiency vs. background expectation.

Figure 5 (from[10]) shows a $Z^\star H \rightarrow \mu^+\mu^- q\overline{q}$ candidate event which has passed all of the selection criteria.

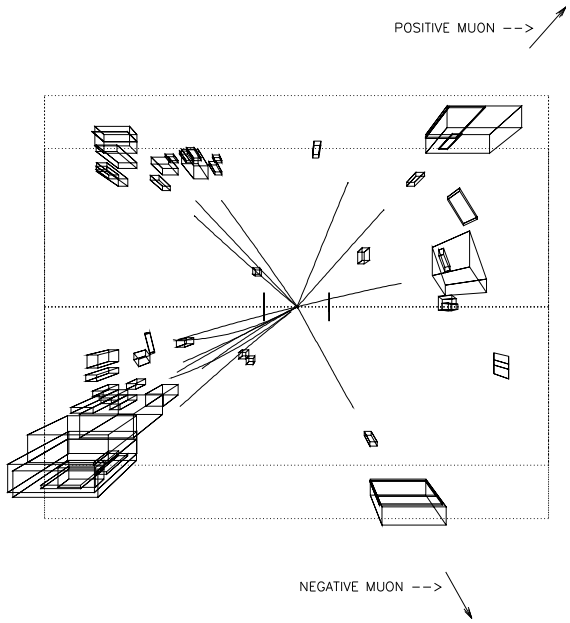

Figure 5. OPAL: Higgs candidate m_H = 61.2 GeV.

Table 2 lists the Higgs boson candidates [9–12] with $m_H > 30$ GeV. The most precise measurement of the mass corresponding to the Higgs candidate mass is calculated from the e^+e^- and $\mu^+\mu^-$ pairs (recoiling mass).

Table 2
MSM Higgs boson candidates.

Experim.	Event Type	Year	Mass (GeV)
ALEPH	$\mu^+\mu^- q\bar{q}$	1993	51.4 ± 0.5
	$\mu^+\mu^- q\bar{q}$	1994	49.7 ± 0.5
	$\mu^+\mu^- q\bar{q}$	1995	66.9 ± 0.3
OPAL	$\mu^+\mu^- q\bar{q}$	1993	61.2 ± 1.0
L3	$e^+e^- q\bar{q}$	1991	31.4 ± 1.5
	$e^+e^- q\bar{q}$	1992	67.6 ± 0.7
DELPHI	$e^+e^- q\bar{q}$	1991	35.9 ± 5.0
(prel.)	$\mu^+\mu^- q\bar{q}$	1993	75.0 ± 0.7

The origin of the event candidates is well understood. They are a result of 4-fermion background. Their production graphs are shown in Fig. 6. Bremsstrahlung (a) and conversion (d) processes are very important when all Higgs boson selection cuts have been applied.

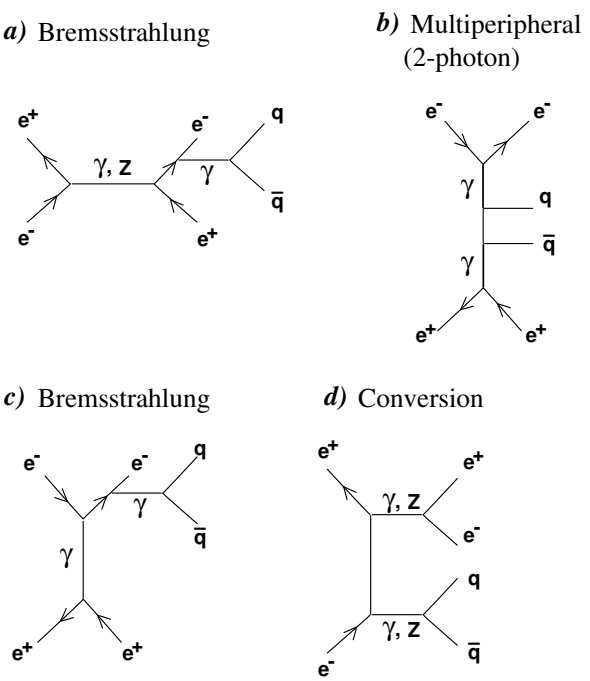

Figure 6. Feynman graphs of 4-fermion background reactions.

The spectrum of the mass recoiling to the lepton pair, corresponding to the Higgs mass, is shown in Fig. 7 (from [11]) before a cut on this variable is applied. The simulated 4-fermion spectrum is in full accordance with the data. Only three out of the thirteen events in the mass region above 50 GeV are likely to be b-flavored and thus selected, as listed in Table 2. About nine 4-fermion events are expected from all four LEP experiments, and eight are observed. It should be noted that about two $\nu\bar{\nu}q\bar{q}$ background events are expected but none are observed. Table 3 summarizes the Higgs mass limits in the MSM [11, 12, 9, 10].

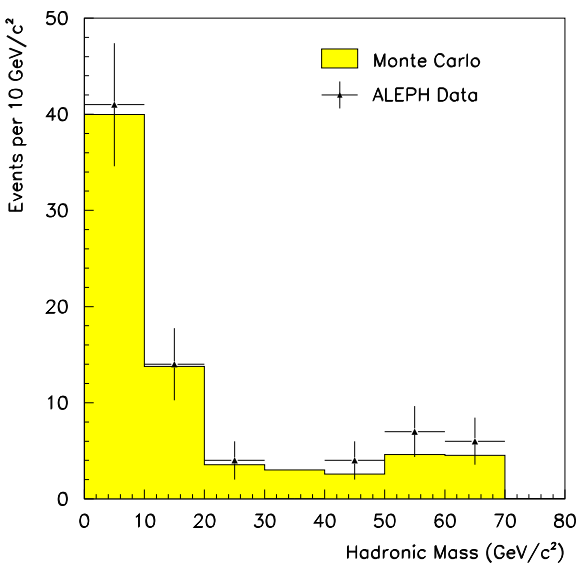

Figure 7. ALEPH: 4-fermion simulation and data.

Table 3
MSM Higgs boson mass limits from ALEPH, DELPHI, L3, and OPAL.

Experiment	ALEPH	DELPHI prel.	L3	OPAL
Data Sample	89-95	90-93	90-94	90-95
$Z \to q\bar{q} \times 10^6$	4.5	1.6	3.1	4.4
Mass Limit				
95%CL (GeV)	**63.9**	**58.3**	**60.2**	**59.6**

The number of expected Higgs events are shown in Fig. 8 (from[10]) for the $\mu^+\mu^-$, e^+e^- and $\nu\bar{\nu}$ channels. The limit is set using Poisson statistics. In a mass region without a Higgs candidate the 95% CL limit is set where the sum of the expected events is three.

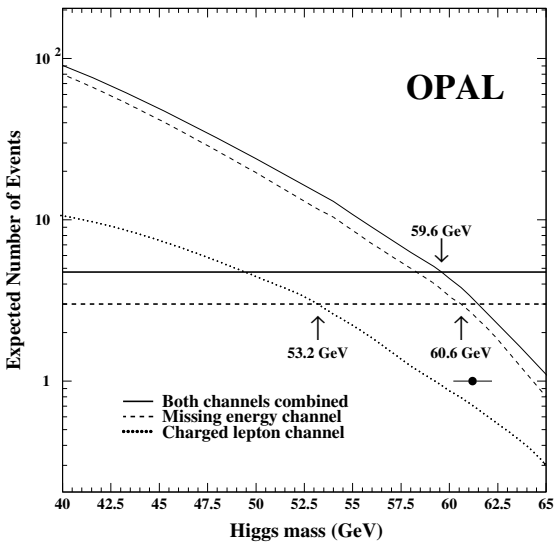

Figure 8. OPAL: Expected MSM events.

2.2. Combined LEP1 Limit

The number of expected events is given for each LEP experiment [11, 12, 9, 10], and shown in Fig. 9 for combined data corresponding to a total of 13.6 million hadronic Z decays. In good approximation, a combined Higgs mass limit can be set by the summation of the number of expected Higgs events. The calculation of the 95% CL limit takes the background events into account and corrects for up to 25% reduction because of tighter selection cuts with increasing statistics. The combined mass limit is 65.6 GeV. Previous limits with this method were reported: 59.3 GeV (1992) [13], 63.5 GeV (1994) [14], and 65.1 GeV (1995) [5]. Figure 9 shows that with larger statistics irreducible 4-fermion background remains and significantly reduces the sensitivity. The microvertex b-quark tagging is crucial to limit the background rate.

The evolution of the published Higgs mass limits is shown in Fig. 10. The sensitivity can be extrapolated assuming 50% efficiency in the $\mu^+\mu^-$, e^+e^- and $\nu\bar{\nu}$ channels. The combined LEP1 limit also lies below the extrapolated line, as all the experiments have adjusted their event selection according to their own maximal visible Higgs mass. The combined mass limits vary only slightly when using other statistical methods under study in the current LEP Higgs working group.

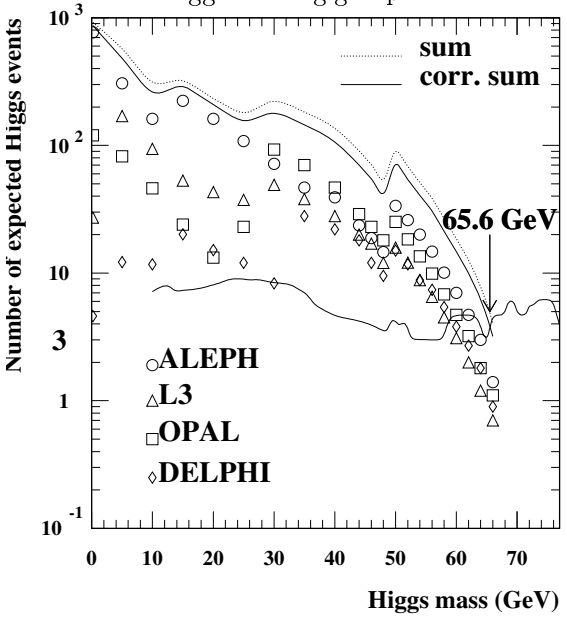

Figure 9. Combined MSM Higgs mass limit from results of ALEPH, DELPHI, L3 and OPAL.

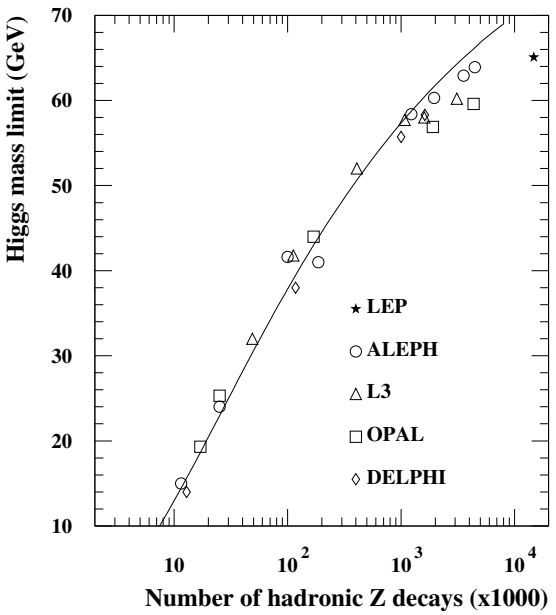

Figure 10. Higgs mass limits and extrapolation of sensitivity.

3. Non-Minimal Higgs Boson Search

There are four classes of searches for non-minimal Higgs bosons: a) searches for Higgs bremsstrahlung with reduced production rates compared to the MSM prediction, b) neutral Higgs pair-production, c) charged Higgs pair-production, and d) Higgs-strahlung off b-quarks or τ-leptons. The production graphs are shown in Fig. 11.

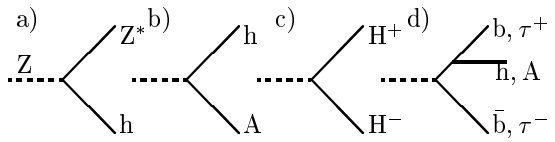

Figure 11. Non-minimal Higgs boson production.

3.1. Invisible Higgs Boson Search

Supersymmetric models with broken R-parity or possible $h \to \chi^0\chi^0$ decays where χ^0 is the lightest Supersymmetric particle predict invisible Higgs decays. Such invisible Higgs bosons are searched for in bremsstrahlung production (Fig. 11a) in analogy with the MSM Higgs boson [11, 12, 9, 10]. The $Z \to e^+e^-$, $\mu^+\mu^-$ and $q\overline{q}$ channels are important. Larger sensitivities are reached compared to the MSM search, as the $Z \to q\overline{q}$ channel gives a clean signature for the invisible Higgs. Interpretations as mass limits are given in Majoron-type models [15] with one Higgs doublet and one Higgs singlet, as shown in Fig. 12 (from [16]) based on [9].

3.2. $Z \to hA$ Search

In the decay channel with four jets a good hadronic mass resolution allows the reconstruction of both of the Higgs masses. Many 4-jet events pass the event-shape and invariant mass selection cuts. A further event selection is based on the fact that Higgs events produce b-flavored jets. These jets can be selected as B mesons have a long lifetime (τ_B = 1.5 ps) and thus a larger number of secondary vertices can be detected. All LEP experiments are equipped with microvertex detectors. These detectors allow b-flavored jets with secondary vertices to be tagged. Figure 13 (from [17]) shows such a bbbb candidate.

All mass combinations up to the kinematic production threshold are scanned. No signal above the QCD background expectations is observed. The limits on $\Gamma(Z \to hA)/\Gamma(Z \to q\bar{q})$ vary with m_h and m_A. These limits are of the order of 10^{-3} to 10^{-4} [18, 17, 19, 20].

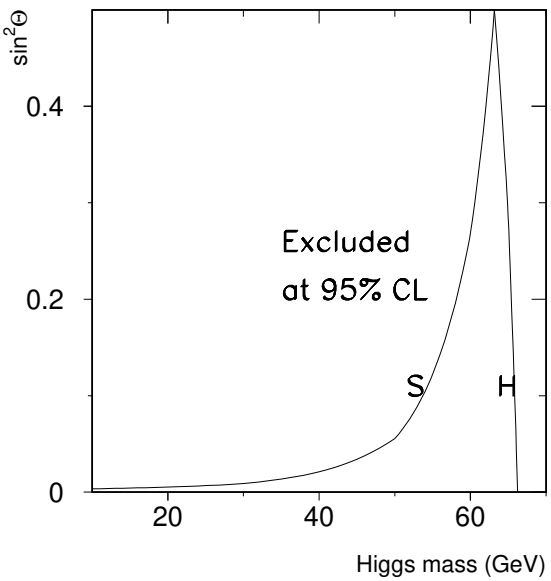

Figure 12. Limits on the masses of invisibly decaying Higgs bosons as a function of the mixing angle $\sin^2\theta$, at 95%CL. S and H are the Higgs bosons in the Majoron model for $r_S = r_H = 0$.

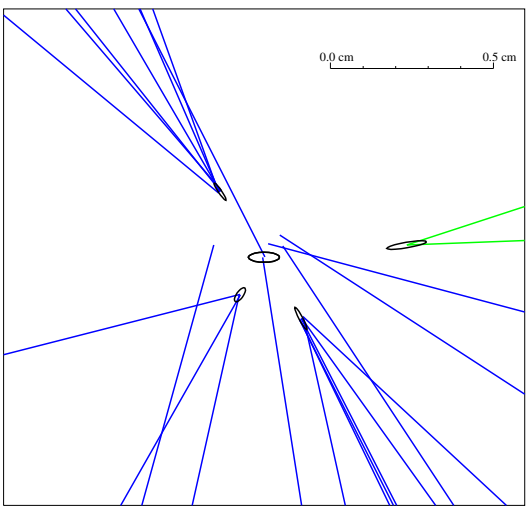

Figure 13. DELPHI: b-jet tagging using a microvertex detector. Central beam position and secondary vertices are marked.

3.3. $Z \to H^+H^-$ Search

For hadronic cscs decays, a similar signature as for the bbbb channel is expected, however, on the one hand, owing to equal H^+ and H^- masses, harder kinematic constraints can be applied, and a charged Higgs mass resolution of about 1 GeV is expected. On the other hand, due to the shorter D-meson lifetime no jet-flavor-tagging can be applied in the cscs channel, and more irreducible background events remain, as shown in Fig. 14 (from [20]).

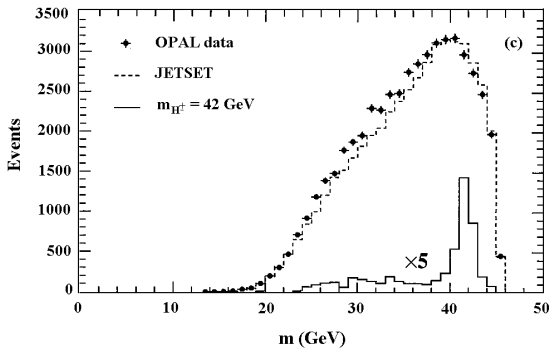

Figure 14. OPAL: cscs invariant mass.

For cs$\tau\nu$ decays, event-shape selection cuts and the requirement of an isolated τ lead to a good background rejection. After all the selection cuts, a Higgs signal would be clearly visible in the reconstructed jet-jet invariant mass distribution.

For $\tau\nu\tau\nu$ decays, a good separation of simulated Higgs signal and $Z \to \tau^+\tau^-$ background can be achieved using the acoplanarity angle.

4. Interpretation in the 2-Doublet Model

Production rates for Higgs boson bremsstrahlung and neutral Higgs boson pair-production are complementary. Therefore, a Higgs boson cannot escape detection if it is kinematically accessible. The search for Higgs bremsstrahlung in the MSM Higgs decay channels with reduced production rates is particularly important. The experimental results set limits on the parameters of the general two-doublet Higgs model.

4.1. Non-Minimal Neutral Higgs Bosons

The combined LEP limit from Higgs boson bremsstrahlung searches in Fig. 9 can be interpreted as a limit on the parameter $\sin^2(\beta-\alpha)$ of the two-doublet Higgs model, shown in Fig. 15.

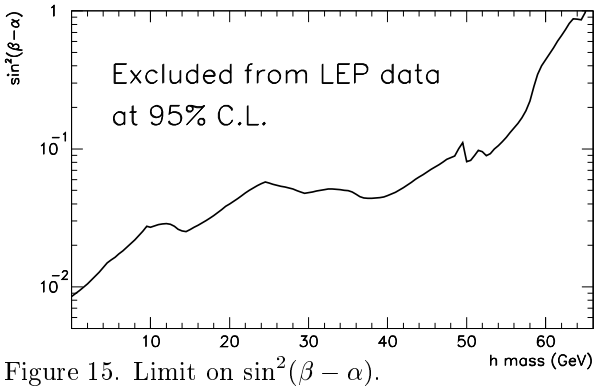

Figure 15. Limit on $\sin^2(\beta-\alpha)$.

The value $\cos^2(\beta-\alpha)$ can be constrained by precision Z-lineshape [21] measurements owing to the large production rate of $Z \to hA$. Any non-minimal MSM contribution to the Z-width larger than 23 MeV is excluded at 95% CL [22]. This value is the result of a comparison of the measurement and theoretical prediction. The production rate of $Z \to hA$ depends on the Higgs boson masses and the $\cos^2(\beta-\alpha)$ value. A limit on $\cos^2(\beta-\alpha)$ is shown in Fig. 16 (from [22]). As a consequence, the combination of sine and cosine limits excludes a large region in the (m_h,m_A) parameter space, as shown in Fig. 17. Figure 18 (from [17]) shows DELPHI limits on (m_h,m_A) from direct searches.

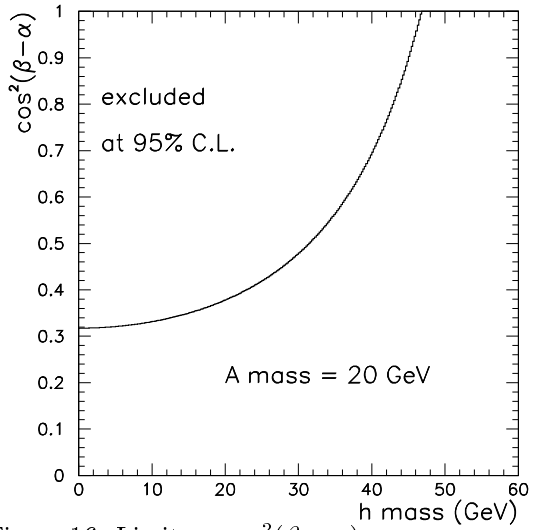

Figure 16. Limit on $\cos^2(\beta-\alpha)$.

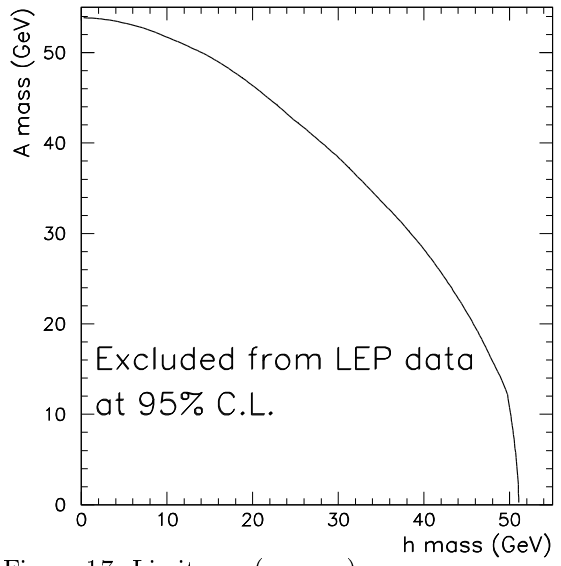

Figure 17. Limits on ($m_{\rm h}$,$m_{\rm A}$).

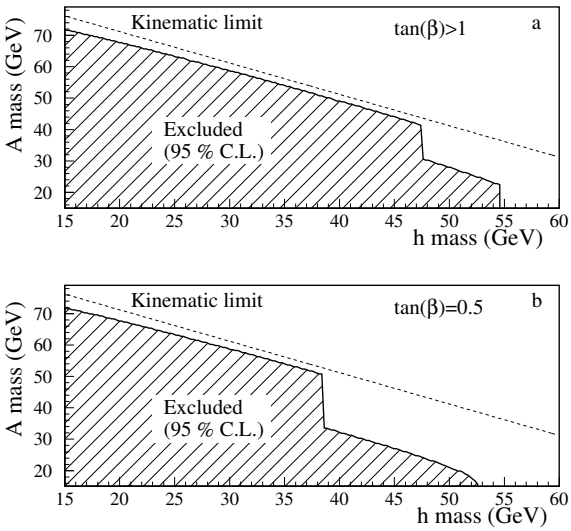

Figure 18. DELPHI: Limits on ($m_{\rm h}$,$m_{\rm A}$).

4.2. Non-Minimal Charged Higgs Bosons

In the two-doublet Higgs model the charged Higgs boson production rate is only a function of the charged Higgs mass [23]. Figure 19 (from [20]) shows 95% CL mass limits on charged Higgs bosons as a function of their leptonic branching ratio obtained from the searches in the cscs, cs$\tau\nu$, and $\tau\nu\tau\nu$ decay channels. Other results are reported in [24, 25, 19].

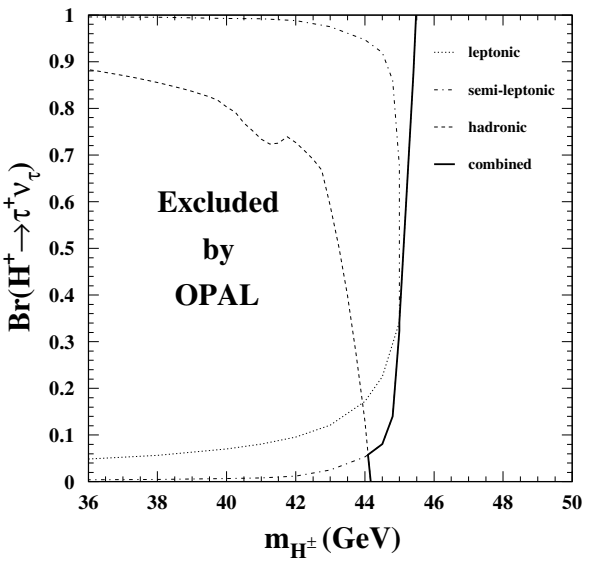

Figure 19. OPAL: Charged Higgs mass limits from direct searches.

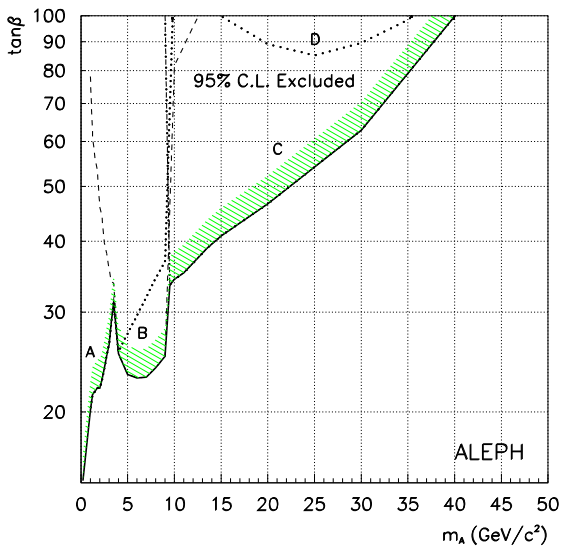

Figure 20. ALEPH: Excluded regions from $e^+e^- \to f\bar{f} \to f\bar{f}A$ searches.

4.3. Bremsstrahlung off b and τ

Previously, limits for the bremsstrahlung process (Fig. 11 d) were reported by L3 [19]. Figure 20 (from [26]) shows results by ALEPH as 95% CL limits in the ($m_{\rm A}$,tan β) plane.

5. Interpretation in the MSSM

The MSSM Higgs boson production rates and decay branching ratios are functions of the Higgs boson masses. When the radiative corrections to the tree-level calculations are included, the production rates and decay branching ratios will also depend on a large number of unknown parameters of the Supersymmetric model [27]. The effect of radiative corrections is illustrated in Fig. 21 (from [28]). Regions are shown where more than 250 $Z \to hA$ events per 1 million hadronic Z decays are expected for a) no, b) small, c) large, and d) very large radiative corrections ($m_{\tilde{t}} = 1$ TeV). Compared to the tree-level calculations (Fig. 21a), the (m_h,m_A) parameter space is largely extended.

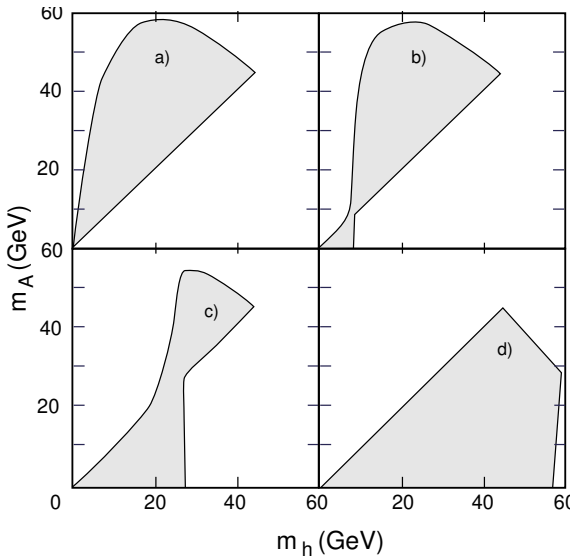

Figure 21. Regions with large $Z \to hA$ production depending on the amount of radiative corrections in the MSSM.

The LEP experiments have interpreted their results as a function of top and stop masses. Figure 22 (from [18, 17, 19, 20]) shows the MSSM results of the four LEP experiments for independent variation over top and stop masses (except DELPHI, which has fixed top and stop masses). An analysis with greater theoretical precision [29] has revealed a new unexcluded mass region as shown in Fig. 23 marked with thick contour lines. Further searches for intermediate-mass Higgs bosons could reduce this region. In addition to $m_{\tilde{t}}$, the effects of other Supersymmetric particles on Higgs boson cross sections and branching ratios are significant. This plot is based on the L3 results [19] given in Fig. 22.

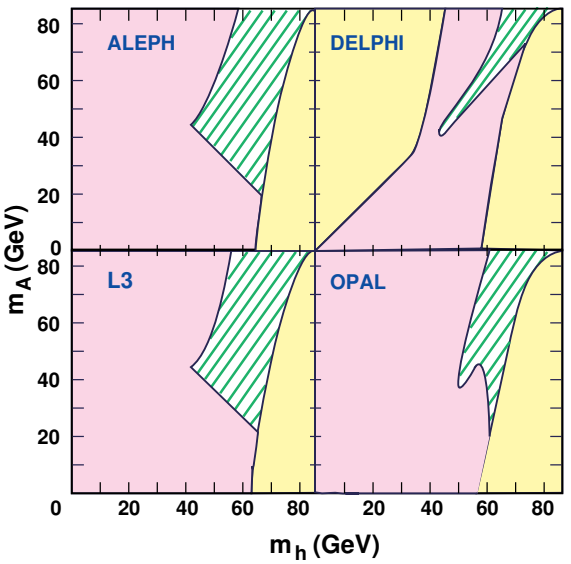

Figure 22. ALEPH, DELPHI, L3, OPAL: MSSM results. The dark region is excluded, the hatched region allowed, and the light region not allowed by the theory.

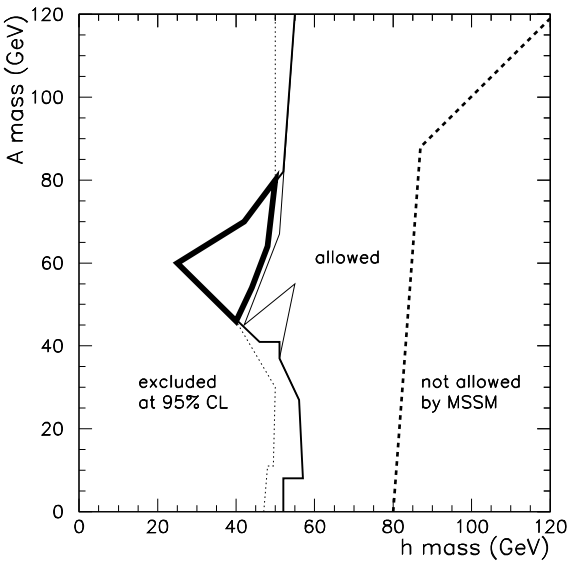

Figure 23. MSSM results with full one-loop radiative corrections.

6. Preliminary LEP2 Results

The prospects of LEP2 are discussed in [30]. The increase of the center-of-mass energy at LEP2 extended the reach of Higgs boson searches. Figure 24 (from [31]) shows the ALEPH mass limit including the data taken at 172 GeV center-of-mass energy. The current expected combined sensitivity is about 77 GeV [30]. In the framework of the MSSM, LEP2 results constrain the parameter region further as shown in Fig. 25 (from [32]).

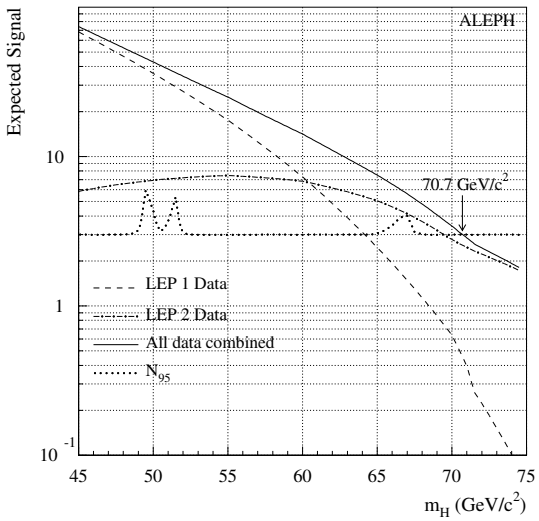

Figure 24. ALEPH: LEP2 MSM limit.

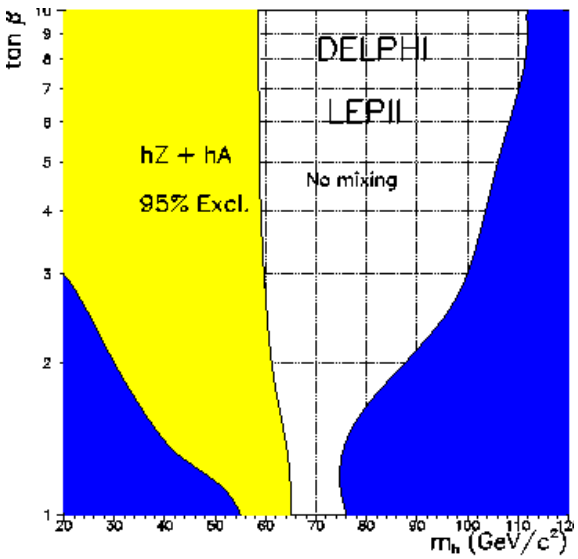

Figure 25. DELPHI: LEP2 MSSM limit.

7. Conclusions

No Higgs boson signal was observed in LEP1 data. The sensitivity for the Higgs boson in the MSM has exceeded expectations. The pre-LEP expectations for the sensitivity range of LEP1 were about 30 GeV [27], while a Higgs mass larger than 60 GeV has already been excluded by individual LEP1 searches. The combined LEP1 limit from the four experiments on the MSM Higgs boson mass is 65.6 GeV at 95% CL.

In the two-doublet Higgs model, searches for neutral and charged Higgs bosons lead to various limits on their production rates. Charged Higgs bosons are excluded independently of the decay mode up to the kinematic reach of LEP1 of about 45 GeV. Mass limits and limits on $\sin^2(\beta-\alpha)$ and $\cos^2(\beta-\alpha)$ are obtained. The large data set is important for the higher sensitivity of Higgs bremsstrahlung production and neutral Higgs pair-production, as both production rates are unpredicted. In the MSSM, LEP1 has almost covered the kinematically accessible parameter mass region and excluded it.

Preliminary LEP2 results are released for the MSM and MSSM Higgs boson search. No indication of a Higgs boson signal has been observed.

The prospects of the MSM Higgs search at LEP2 will predominantly depend on the achievable center-of-mass energy. The MSM Higgs boson reach will be 90 to 100 GeV. With a large center-of-mass energy almost the entire allowed ($m_{\rm h}$,$m_{\rm A}$) parameter space of the MSSM will be accessible. The sensitivity mass range for a charged Higgs boson depends largely on the total integrated luminosity, and will extend to about 70 GeV for $\mathcal{L} = 500$ pb^{-1} [33, 30].

Acknowledgements

I would like to thank my fellow Higgs hunters for many fruitful discussions, my Indian colleagues for their warm hospitality, and last but not least Andrey Kunin, Wolfgang Lohmann, and Hannelies Nowak for their comments on the manuscript.

REFERENCES

1 LEP Experiments Committee, 45th meeting, CERN/LEPC 97-4.

2 P.W. Higgs, *Phys. Lett.* **12** (1964) 132;
P.W. Higgs, *Phys. Rev. Lett.* **13** (1964) 508;
P.W. Higgs, *Phys. Rev.* **145** (1966) 1156;
F. Englert and R. Brout, *Phys. Rev. Lett.* **13** (1964) 321;
G.S. Guralnik, C.S. Hagen and T.W.B. Kibble, *Phys. Rev. Lett.* **13** (1964) 585.

3 LEP Lineshape Working Group, contrib. to the Moriond conf. 1997;
A. Gurtu, *Phys. Lett.* **B 385** (1996) 415.

4 E. Gross, Talk at the Moriond conf. 1997, to be published in the proceedings.

5 A. Sopczak, Preprint CERN, PPE/95-46 (1995); hep-ph/9504300; Proc. IX Int. Workshop on High Energy Physics, Moscow, Russia, (1994) ISBN 5-211, p. 88.

6 F. A. Berends and R. Kleiss, *Nucl. Phys.* **B 260** (1985) 32.

7 B.L. Ioffe and V.A. Khoze, Preprint LINP, Leningrad, Nov. 1976;
J.D. Bjorken, Proc. of the 1976 SLAC Summer Institute on Particle Physics, Stanford, ed. M.C. Zipf (SLAC, Stanford, 1977) p. 1.

8 B.A. Kniehl, *Z. Phys.* **C 55** (1992) 605;
A. Denner *et al.*, *Z. Phys.* **C 56** (1992) 261.

9 L3 Coll. M. Acciarri *et al.*, *Phys. Lett.* **B 385** (1996) 454.

10 OPAL Coll., M.Z. Akrawy *et al.*, *Phys. Lett.* **B 327** (1994) 397; *Phys. Lett.* **B 377** (1996) 273; *Z. Phys.* **C 73** (1997) 189.

11 ALEPH Coll., D. Buskulic *et al.*, *Phys. Lett.* **B 313** (1993) 299; *Phys. Lett.* **B 384** (1996) 427.

12 DELPHI Coll., P. Abreu *et al.*, *Nucl. Phys.* **B 373** (1992) 3; *Nucl. Phys.* **B 421** (1994) 3; contrib. to the Warsaw conf. 1996 (DELPHI note 96-85).

13 A. Sopczak, Preprint CERN, PPE/92-137 (1992); Proc. XV Int. Meeting on Particle Physics, Kazimierz, Warsaw, Poland, 25-29 May 1992, *World Scientific* (1993), p. 45.

14 A. Sopczak, Preprint CERN, PPE/94-73 (1994); Proc. Int. Lisbon Fall School 1993, Nucl. Phys. B Proc. Suppl. **C 37** (1995) p. 168.

15 Y. Chikashige, R.N. Mohapatra, R.D. Peccei, *Phys. Lett.* **B 98** (1980) 265;
R.E. Shrock, M. Suzuki, *Phys. Lett.* **B 10** (1982) 250;
R. Mohapatra, J.W.F. Valle, *Phys. Rev.* **D 34** (1986) 1642;
A. Zee, *Phys. Lett.* **B 93** (1980) 389.

16 S. Mangla, PhD Thesis 1997 (in prep.).

17 DELPHI Coll., P. Abreu *et al.*, *Z. Phys.* **C 67** (1995) 69; contrib. to the Warsaw conf. 1996 (DELPHI note 96-85).

18 ALEPH Coll., D. Buskulic *et al.*, *Phys. Lett.* **B 313** (1993) 312.

19 L3 Coll., O. Adriani *et al.*, *Z. Phys.* **C 57** (1993) 355.

20 OPAL Coll., P.D. Acton *et al.*, *Phys. Lett.* **B 265** (1991) 475; *Z. Phys.* **C 64** (1994) 1;
Phys. Lett. **B 370** (1996) 174.

21 LEP Experiments, Preprint CERN, PPE/94-187 (1994).

22 A. Sopczak, *Mod. Phys. Lett.* **A 10** (1995) 1057.

23 S. Komamiya, *Phys. Rev.* **D 38** (1988) 2158.

24 ALEPH Coll., D. Decamp *et al.*, *Phys. Lett.* **B 241** (1990) 623.

25 DELPHI Coll., P. Abreu *et al.*, *Z. Phys.* **C 64** (1994) 183.

26 ALEPH Coll., contrib. to the Warsaw conf. 1996, (PA13-027).

27 J.F. Gunion, H.E. Haber, G.L. Kane and S. Dawson, "The Physics of the Higgs Bosons: Higgs Hunter's Guide", *Addison Wesley*, Menlo Park, (1989).

28 A. Sopczak, "Search for Non-minimal Higgs Bosons from Z Decays with the L3 Experiment at LEP", Ph.D. Thesis, U. of Cal., San Diego, 1992.

29 J. Rosiek and A. Sopczak, *Phys. Lett.* **B 341** (1995) 419.

30 E. Accomando *et al.*, "Higgs Physics" Physics at LEP2, CERN Yellow Report CERN 96-01 (1996).

31 ALEPH Coll., contrib. to the Moriond conf. 1997.

32 DELPHI Coll., contrib. to the Moriond conf. 1997.

33 A. Sopczak, *Int. J. Mod. Phys.* **A9** (1994) 1747.